Third International Conference on Advanced Science and Engineering (ICOASE2020)
University of Zakho, Duhok Polytechnic University, Kurdistan Region, Iraq

COVID-19 Diagnosis from Chest X-ray Images Using Deep Learning Approach

Noor N. Qaqos
IT Department
Duhok Polytechnic University Duhok, Kurdistan Region,Iraq
noor.qaqos@dpu.edu.krd

Omar S. Kareem
IT Department
Duhok Polytechnic University
Duhok, Kurdistan Region, Iraq
omar.kareem@dpu.edu.kr

2020 International Conference on Advanced Science and Engineering (ICOASE) | 978-1-6654-1579-8/20/$31.00 ©2020 IEEE | DOI: 10.1109/ICOASE51841.2020.9436614

***Abstract*— Coronavirus (COVID-19) disease is an infectious disease caused by the newly and deadly pneumonia type identified Coronavirus2 (SARS-CoV-2). A real-time Reverse Transcription Polymerase Chain Reaction (RT-PCR) is the main method and has been regarded as the gold standard for diagnosing the COVID-19. Strict requirements and the limited supply of RT-PCR kits for the laboratory environment leads to delay in the accurate diagnosis of patients in addition to the test takes 4-6 hours to obtain the results. To tackle this problem, radiological images such as chest X-rays and CT scan could be the answer to test the COVID-19 infection rapidly and more efficiently. In this paper, an efficient proposed Convolution Neural Network (CNN) architecture model for COVID-19 detection based on chest X-ray images is presented. The proposed model is developed to provide accurate detection for binary classification (Normal vs. COVID-19), three class classification (Normal vs. COVID-19 vs. Pneumonia), and four class classification (Normal vs. COVID-19 vs. Pneumonia vs. Tuberculosis (TB)). Our proposed model produced an overall testing accuracy of 99.7%, 95.02%, and 94.53% for binary, three, and four class classifications, respectively. A comparison is made between this work and others shows the superior of this work over the others.**

Keywords: COVID-19, Diagnosis, Deep Learning, CNN, Chest, X-ray images.

I. INTRODUCTION

COVID-19 is a novel strain of coronavirus (SARS-CoV-2). It has caused a devastating influence on daily lives and the health public. It has a fatal nature by threatening the respiratory systems and damage the health of millions of people across the world until recent times [1]. Many hypotheses assumed that this virus had been originated from animals. However, till now the source of this virus has not been identified [2]. It launched in Wuhan city of Hubei province in China on December 31, 2019, as a pneumonia-like infection due to an observation of an unknown cause among people related to the respiratory system, within a short period the disease expanded to all other parts of the world and the World Health Organization (WHO) was classified it as a pandemic. The most common symptoms that appear in the COVID-19 patient are fever, cough, sore throat, and difficulty in breathing. Other symptoms can also be noticed in some patients represent by vanishing of sense of smell, taste, tiredness, aches, and nasal blockage [3, 4, and 5]. The coronavirus has infected millions of people and the number of deaths is increasing day by day. Droplets of saliva by coughing and sneezing from COVID-19 patients is the main reason for spreading the virus [1]. The number of people that have been infected and died in the whole world until the time of writing this article is 55.2 and 1.33 million, respectively. Early and accurate diagnosis of Coronavirus is one of the first importance for controlling the spread of the disease and to reduce the number of deaths [2].

With the rapid development of computer technology and its applications. In recent times, deep learning approaches represent one of the most techniques that have had successful applications to resolve many problems and especially in medical imagining. Therefore, accurate, precise, and faster intelligence detection systems may support to overcome this problem in the rapid rise of the COVID-19 epidemic [6]. Deep learning approaches such as CNN architectures represent one of the most common techniques with superior achievements in the field of medical imaging applications [7]. Deep CNNs are utilize for automatic feature extraction, which is achieved by a process called convolution. Each layer involves a transformation of the data into a higher and more abstract level. CNN has been considered as one of the most important algorithms in the fields of computer vision and medical imaging. Since lungs are the primary target of COVID-19, analyzing and examining their changes by CNN approaches can give an explicit result for the presence of the virus [8]. In this work, we preferred two things for COVID-19 detection: Firstly, radiological images (X-ray and CT images) over the RT-PCR test due to in RT-PCR test the time for spreading Coronavirus among people takes more time to generate the result. Secondly, pulmonary X-rays over CT images because X-ray machines are available in most of the health cares. The main target of this paper is to propose an efficient CNN architecture model to detect and classify COVID-19 cases for high accuracy. The main contribution and advantages of our proposed model can be summerized as follows:

- The model performs a good diagnosis of COVID-19 cases.
- The model successfully classifies the mentioned four classes with an accuracy= 99.7, 95.02, and 94.53 on testing dataset for binary, three and four class classification.
- The comparison in section VI shows the proposed CNN architecture outperforms the alternative other works.

This paper is organized as follows: Besides this introductory section, Section II describes the related works of COVID-19 detection using deep learning approaches. Material and methodology including the chest X-ray dataset and the proposed CNN model are introduced in section III. Experimental results based on evaluation metrics to measure the performance, training, and testing of the model on the anaconda environment are presented in section IV. Section V compares our achieved results with other previous works. Finally, conclusions are drawn based on our results.

II. RELATED WORKS

In this section, we introduce some of the previous works of using deep learning techniques. Convolutional neural network has been used by many scientists to diagnose COVID-19 from different pulmonary images. Rahimzadeh et al. [9] proposed a concatenation of two neural networks (Xception and ResNet50V2) to classify chest X-ray images into three class classification Normal, COVID-19 and Pneumonia. They concluded that the proposed model achieved an overall average accuracy of 91.4%. DarkNet presented as a new model by Ozturk et al.[10] for automatic COVID-19 detection. The model produced a classification accuracy of 98.08% and 87.02% for binary classes and multi-class classification, respectively. Alom et al. [11] applied NABLA-3 network models to improve the Inception of Recurrent Residual Neural Network (IRRCNN). Ahuja et al. [12] evaluated the performance of four well-known pre-trained CNN architectures. The results showed that ResNet18 pre-trained model performs better classification accuracy than others. Loey et al. [13] compared the performance of five various deep CNN models for COVID-19 cases detection Results showed that ResNet50 is the most efficient deep learning model. Sarker et al. [14] proposed a deep learning-based approach to effective detection of COVID-19 patients using Densenet-121. Asif et al. [15] proposed a DCNN based model Inception V3 with incorporated transfer learning to detect COVID-19 cases using chest X-ray images. Al-Timemy et al. [16] compiled a five-class dataset of chest X-ray images consisting of a balanced number of COVID-19 cases, viral Pneumonia, bacterial Pneumonia, TB, and healthy cases. The comparison showed that a pipeline of ResNet-50 for DF computation is the best classifier. A Deep CNN model (CoroNet) based on the Xception architecture pre-trained model for automatic detection of COVID-19 infection from pulmonary X-ray images proposed by Khan et al. [17]. Panwar et al. [8] proposed a deep learning neural network-based method (nCOVnet) with the transfer learning model and they obtained training accuracy and training loss of 97% and 0.2%, respectively. Abbas et al. [7] proposed a deep CNN architecture model, DeTraC, for COVID-19 classification cases using a pulmonary X-ray image. The experimental results indicated the capability and high performance of the used model. Apostolopoulos et al. [18] evaluated the performance of CNNs for medical image classification. Five different pre-trained CNN models for the detection of COVID-19 used by Narin et al. [19]. Toraman et al. [20] proposed an accurate and fast approach to diagnose COVID-19 [24-25].

III. MATRERIAL AND METHODS

A. *Chest X-ray image Dataset*

We have used two open sources of datasets in this work. The original dataset is taken from the Kaggle repository [21].

TABLE I: DETAILS OF TRAINING, VALIDATING, AND TESTING DATASET.

Chest X-ray images	Number of images	Training (70%)	Validation (15%)	Testing (15%)
Normal [21]	1583	1109	237	237
COVID-19 [21]	576	404	86	86
Pneumonia [21]	4273	2991	641	641
Tuberculosis [22]	155	107	24	24
Total images	6587	4611	988	988

This dataset consists of three types of chest X-ray images (Normal, COVID-19 and Pneumonia) from different healthy and patient people and it used for binary and three class classifications. The tuberculosis chest X-ray images dataset is taken from another resource [22]. We merged these two datasets for four-class classification. The overall datasets are divided into three folders (training, validating and testing); each of them contains four sub-folders (normal, COVID-19, Pneumonia and Tuberculosis). The whole datasets are divided based on ratios 70:15:15 as training, validating, and testing, respectively. A total of 6587 images are used and partitioned and the details are listed in the table I.

B. *Proposed CNN Architecture model*

The overall proposed CNN architecture model is shown in Fig. 1. Since the dataset used was composed of pulmonary images having heterogeneous, different, and larger sizes ranging from about 510×600 to 3100×2100 pixels; and to deal with reasonable computation time during experiments and training the proposed CNN model, all chest X-ray images were down sampling (resized) from their original size to a unique dimension and rescaled into smaller images (128×128 pixels) to fit with standard inputs of the model. The model comprised of two basic parts: the feature extractor and classifier illustrated as follows:

1- *Feature Extractor*

Each layer of the feature extractor takes its input from the outputs of the intermediate preceding, and its output is passed as an input to the succeeding other layers. The proposed architecture in Fig. 1 comprised of convolution, max pooling, batch normalization, dropout, and classification layers combined together. The feature extractor comprises of 4 Conv blocks of layers: conv block#1 3×3, 32; conv block#2 3×3, 64; conv block#3 3×3, 128 and conv block#4 3×3, 256, where 3×3 is the filter size (kernel) used with convolution process and 32, 64, 128 and 256 are the number of filters used in each conv block# 1,2,3 and 4 respectively.

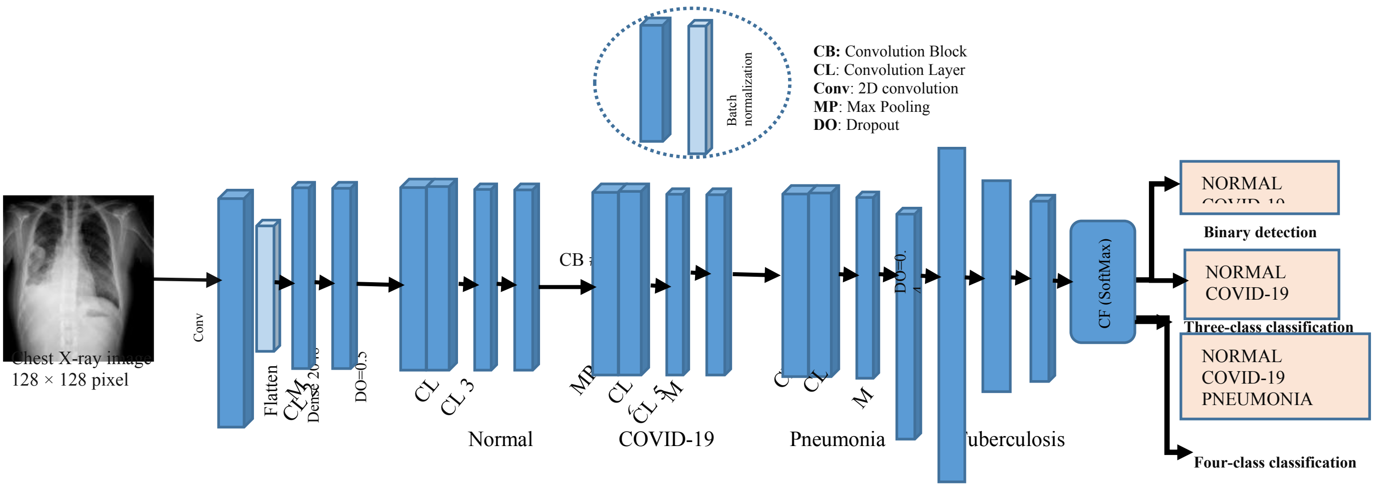

Fig. 1. Proposed CNN architecture Model

Each block consists of 2 conv layers, batch normalization is used between layers, and it is a technique that used to improve the convergence during model training. Max pooling layer used between conv blocks and dropout rate with values 0.1, 0.2, 0.3 and 0.4 is used between blocks#1,2,3 and 4, respectively. Dropout is a regularization technique for neural network models where randomly selected neurons are ignored during training. The output of max-pooling operations between conv blocks are gathered into 2-D planes called feature maps, and we obtained 64×64×32, 32×32×64, 16×16×128, 8×8×256, for output of block #1, 2, 3, and 4, respectively. Rectified Linear Units (ReLUs) are used and applied as an activation function to all convolution layers that have output 0 if the input is less than 0 and the output is the same input otherwise. The same padding process is also used to ensure that the output has the same shape as the input data.

2- A classifier

The classifier is simply an Artificial Neural Network (ANN). It is placed at the end of CNN model, often referred to dense layer. It requires an individual features (vectors) as an input to accomplish the computations and to fix its parameters through training operation. Therefore, the output of the feature extractor is transformed to a vector of 1-D and used it as an input to a classifier. This process is called flattening, where the output of the convolution layers operation is flattened to produce one lengthy vector for the dense layer to employ in its final classification process. In the proposed model, the classifier part consists of a flatten layer, one dense layer, and a dropout operation of size 0.5 to classify an input image. SoftMax functions used to perform the binary and multi-class classifications. Table II shows a summary of the proposed CNN architecture model.

IV. Experimental Results

A. Environment

A desktop computer with Microsoft Windows 10 pro-64-bit was used in this experiment. It has the following specifications: Intel Core™ i7-8700 3.2-GHz processor (12 CPUs), 8 GB of DDR4 RAM, 512 GB of a hard disk and GPU NVidia card of 4 Giga. We installed the anaconda

python 3.7 as a software machine tool for simulation. We have done a new environment and installed many libraries such as Keras, TensorFlow, Matplotlib, Cv2, NumPy, Pandas, Python, Scikit, SciPy.

B. Evaluation Metrics

To evaluate and assess the performance and reliability of the proposed model-based classification, we used the same metrics that adopted by [9] and considered the standard metrics as follows:

- ❖ $Accuracy = \frac{Number\ of\ correct\ classified\ images}{Number\ of\ entire\ images}$
- ❖ $= \frac{(TP+TN)}{(TP+TN+FP+FN)}$
- ❖ $Precision = TP/((TP+FP))$
- ❖ $Sensitivity = TP/((TP+FN))$
- ❖ $Specificity = TN/((TN+FP))$
- ❖ $F1\_score = 2(\frac{(precision \times sensitivity)}{(precision + sensitivity)})$

where:

- ➢ TP is the proportion of positive COVID-19 chest X-ray images that were correctly labelled as positive.
- ➢ FP is the proportion of negative (healthy) COVID-19 chest X-ray images that were mislabeled as positive.
- ➢ TN is the proportion of negative (healthy) chest X-ray images that were correctly labelled as healthy.
- ➢ FN is the proportion of positive COVID-19 chest X-ray images that were mislabeled as negative (healthy).

TABLE II: LAYERS AND THEIR PARAMETERS FOR THE PROPOSED MODEL

Layer (type)	Output Shape	Param #
conv2d_1 (Conv2D)	(None, 128, 128, 32)	896
batch_normalization_1 (Batch)	(None, 128, 128, 32)	128
conv2d_2 (Conv2D)	(None, 128, 128, 32)	9248
batch_normalization_2 (Batch)	(None, 128, 128, 32)	128
max_pooling2d_1 (MaxPooling1)	(None, 64, 64, 32)	0
dropout_1 (Dropout)	(None, 64, 64, 32)	0
conv2d_3 (Conv2D)	(None, 64, 64, 64)	18496
batch_normalization_3 (Batch)	(None, 64, 64, 64)	256
conv2d_4 (Conv2D)	(None, 64, 64, 64)	36928
batch_normalization_4 (Batch)	(None, 64, 64, 64)	256
max_pooling2d_2 (MaxPooling2)	(None, 32, 32, 64)	0
dropout_2 (Dropout)	(None, 32, 32, 64)	0
conv2d_5 (Conv2D)	(None, 32, 32, 128)	73856
batch_normalization_5 (Batch)	(None, 32, 32, 128)	512
conv2d_6 (Conv2D)	(None, 32, 32, 128)	147584
batch_normalization_6 (Batch)	(None, 32, 32, 128)	512
max_pooling2d_3 (MaxPooling3)	(None, 16, 16, 128)	0
dropout_3 (Dropout)	(None, 16, 16, 128)	0
conv2d_7 (Conv2D)	(None, 16, 16, 256)	295168
batch_normalization_7 (Batch)	(None, 16, 16, 256)	1024
conv2d_8 (Conv2D)	(None, 16, 16, 256)	590080
batch_normalization_8 (Batch)	(None, 16, 16, 256)	1024
max_pooling2d_4 (MaxPooling4)	(None, 8, 8, 256)	0
dropout_4 (Dropout)	(None, 8, 8, 256)	0
flatten_1 (Flatten)	(None, 16384)	0
dense_1 (Dense)	(None, 2048)	33556480
dropout_5 (Dropout)	(None, 2048)	0
dense_2 (Dense)	(None, 2)	4098
Total params: 34,736,674 Trainable params: 34,734,754 Non-trainable params: 1,920		

V. TRAINING, TESTING AND PERFORMANCE EVALUATION

As mentioned before, our model was trained for 100 epochs using a dataset partitioned into ratios of 75%, 15%, and 15% for training, validation and testing parts, respectively, by using the model introduced in Section III. Fig. 2 shows some randomly selected samples of chest X-ray images prepared dataset after resizing the images to 128×128 pixels. The model was executed and conducted by experiments many times by using anaconda python 3.7 environments using Keras and TensorFlow libraries. Parameters and hyper-parameters were heavily tuned and turned for high accuracy and low loss.Various performances were obtained from the model, but this work reports only the most valid one. The training parameters of the proposed CNN architecture in this study are the learning rate $=e^{-3}$, momentum = 0.9, the values of batch size set to 64 to avoid overfitting and to achieve high accuracy while the number of epochs is set to 100. The deep network classifier is trained using Stochastic Gradient Descent (SGD) because of its good converge and fast running time. Categorical cross-entropy is used as a loss function for pixel-wise binary and multi-class classifications. The classification system was trained and tested on the collected data.

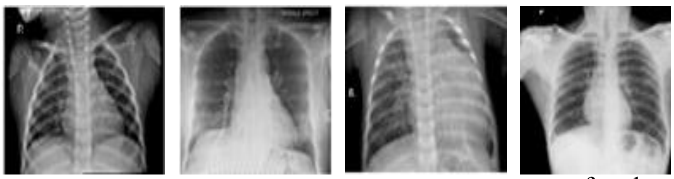

Fig. 2. Some of the random selected samples of four used cases after the down sampling process to 128 × 128 pixels.

The weights of the proposed CNN model were randomly initialized during the training phase of the experiment. The training and validation data results are shown in Fig. 4. As we can easily observe from the Fig. (4a and b) of binary class classification, the validation loss is slowly falling, and the validation accuracy is rapidly increased throughout the whole training whereas there is no major change between training and validation loss accuracy after the 100th epoch. Moreover, the difference between training and validation loss and accuracy is about (loss=0.18, accuracy = 0.05) for three class and it is about (loss=0.19, accuracy = 0.05) for four class classifications without using any image data augmentation in this study. Once the proposed CNN model has been trained using the training set, it is used to diagnose the chest X-ray on the testing dataset.

The performance of the proposed CNN architecture model was measured for each classification using Confusion Matrix (CM) and the metrics illustrated in section IV: accuracy, precision, sensitivity, specificity, and F1-score. Table III shows the overall metrics computed for each class (Normal, COVID-19, Pneumonia, and Tuberculosis), in addition to the overall accuracy of the system. Also, to predicts the different samples of chest X-ray images, a CM is used with four parameters: TP, FP, TN, and FN, as shown in Fig. 4. It can be seen from the CM illustrated in Fig. (3-a) that the proposed model has detected in binary class classification 85 out of 86 patients with COVID-19 as having COVID-19, 237 out of 237 normal patients as normal; and it mislabeled one COVID-19 as a normal patient. In three-class classification, as shown in Fig. 3-b, the proposed model has detected 74 out of 86 patients with COVID-19 as having COVID-19, 229 out of 237 normal patients as normal, 613 out of 641 Pneumonia patients as Pneumonia. The system misclassified 12 COVID-19 patients, five of them as having normal and seven as Pneumonia, 8 patients with normal, one of them as having COVID-19 and the other seven as Pneumonia, 28 patients with Pneumonia as normal. For the confusion matrix of four class classification as shown in Fig. (3-c), the proposed model has detected 69 out of 86 patients with COVID-19 as having COVID-19, 215 out of 237 normal patients as normal, 628 out of 641 pneumonia patients as Pneumonia and 22 out of 24 as tuberculosis. Also, it misclassified 14 patients with COVID-19 were four of them as having normal, twelve as having Pneumonia and one as tuberculosis, 13 with normal patients, one of them as having COVID-19 the other 12 as Pneumonia, 13 patients with pneumonia patients as having normal, two tuberculosis patients as COVID-19. It can be seen that the model predicts the used samples of binary detection with high accuracy and low loss, but the accuracy of other classification is lower than binary detection due to similarities among images of COVID-19, Pneumonia, and Tuberculosis.

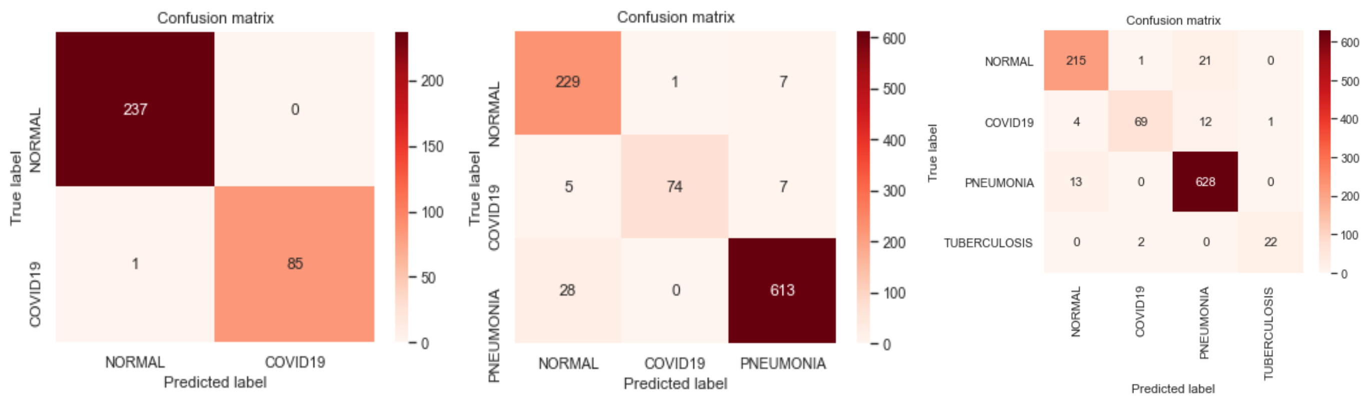

(a) (b) (c)

Fig. 3. Confusion matrix for the proposed system on the testing set (a) Binary class CM (b) three class CM (c) four class CM

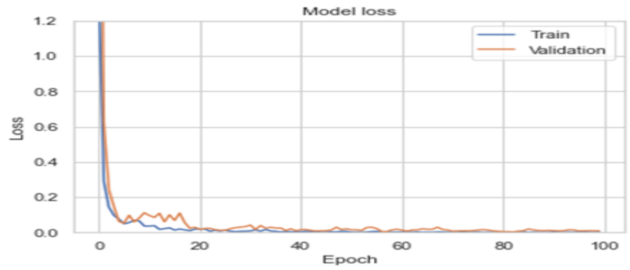

(a)

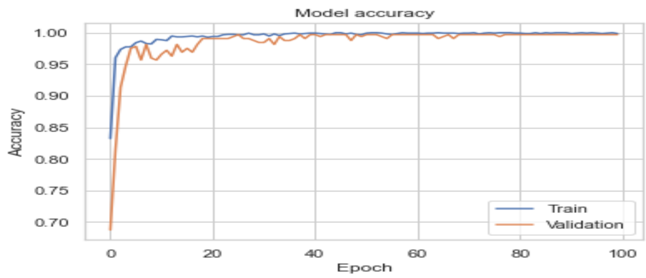

(b)

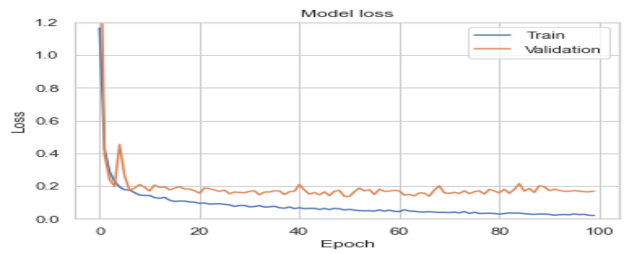

(c)

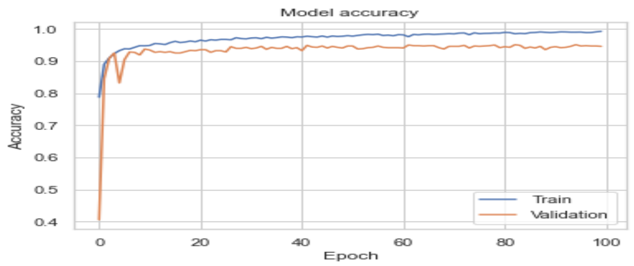

(d)

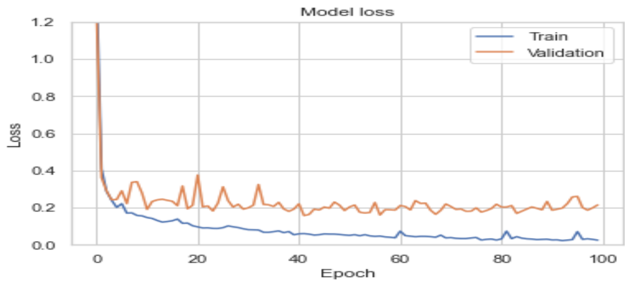

(e)

(f)

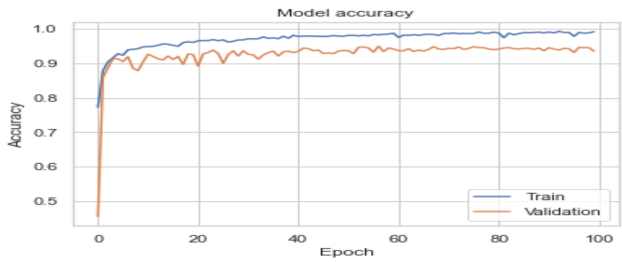

Fig. 4. Training and validation accuracy and loss for (a-b) binary class, (c-d) three class and (e-f) four-class classification.

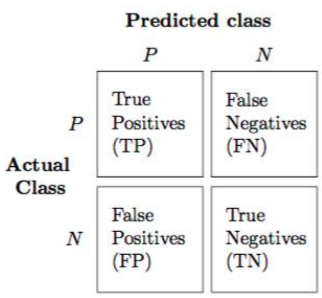

Fig. 5. Confusion Matrix

TABLE III: PRECISION, SENSITIVITY, SPECIFICITY, F1-SCORE, AND OVERALL ACCURACY FOR NORMAL, COVID-19, PNEUMONIA, AND TUBERCULOSIS CLASSES OF THE PROPOSED CNN MODEL

Classifier	Case types	Metrics (%)				
		Precision	sensitivity	F1-score	specificity	System accuracy on the testing dataset
Binary classes	**Normal**	99.57	100	99.78	98.83	**99.7**
	COVID19	100	98.84	99.4	100	
Three classes	**Normal**	87.4	96.62	91.77	95.4	**95.02**
	COVID19	98.66	86.04	91.91	97.22	
	PNEUMONIA	97.76	95.63	96.67	95.58	
Four classes	**Normal**	92.67	90.71	91.67	97.69	**94.53**
	COVID19	95.83	80.23	87.33	99.65	
	PNEUMONIA	95	97.97	96.46	90.26	
	TUBERCULOSIS	95.65	91.66	93.61	99.88	

From Table III, it can be seen that the values of precision and specificity of COVID-19 are 100 % for binary class classification while the sensitivity and F1-score are 98.84 and 99.4, respectively. Whereas, the metrics values of normal class ranging from 99.57 to 100%. For three classes, the values of precision, sensitivity, F1-score, and specificity for COVID-19 are 98.66, 86.04, 91.91, and 97.22, respectively. The other values of normal and Pneumonia cases approximately ranging from 95 to 99 except a precision and F1-score values of normal cases which are equal to 87.4 and 91.77, respectively. The precision, sensitivity, F1-score, and specificity for COVID-19 patients of four classes are equal to 95.83, 80.23, 87.33, and 99.65, respectively, and the other values of metrics ranging from 90.26 to 99.88.

VI. COMPARISON WITH OTHER WORKS

As we quantified the performance of our proposed CNN architecture, we then analyzed the reported performance results from various other research groups, as shown in Table IV. It should be observed that each model tested with a different dataset, different testing split, and also different classes. Hence, the comparison between our work with previous works here is for illustrative purposes, but it shows the potential of our approach over others.

I. CONCLUSIONS AND FUTURE WORK

In this paper, an efficient proposed CNN architecture model is presented. The proposed model is used to detect COVID-19 cases based on chest X-ray images. The main target of our proposed system is to provide accurate detection for binary classification (Normal (healthy) vs. COVID-19), three class classification (Normal vs. COVID-19 vs. Pneumonia), and four class classification (Normal vs. COVID-19 vs. Pneumonia vs. Tuberculosis). Our model has been trained and tested on a dataset that are publicly available from Kaggle respiratory. The classification efficiency was evaluated and measured using five metrics: accuracy, precision, sensitivity, F1-score, and specificity. The proposed model produced an overall testing accuracy of 99.7%, 95.02%, and 94.53% for binary, three, and four class classifications, respectively. Comparative analyses reveal the proposed model outperforms other alternative works. Therefore, the proposed model can help clinicians to detect COVID-19 cases more accuracy. In the near future research direction, we intend to detect and classify other lung diseases that are not mentioned in this work based on our proposed CNN architecture model.

TABLE IV: COMPARISON OF THE PROPOSED MODEL WITH OTHER DEEP LEARNING APPROACHES DEVELOPED

References	Types of chest images	Number of cases	Number of classes	Methodology	Testing Accuracy (%)
Ref [6]	CT scan	Normal=175 COVID19=219 Influenza-A viral PNEUMONIA=224	3	Deep learning system	86.7
Ref [7]	Chest X-ray	Normal=80 COVID19=116	2	DeTraC + deep CNN	93.1
Ref [8]	Chest X-ray	Normal=142 COVID19=142	2	nCOVnet CNN	88
Ref [9]	Chest X-ray	Normal=8851 COVID19=180 PNEUMONIA=605 4	3	Concatenation of Xception and ResNet50v2	91.4
Ref [10]	Chest X-ray	Normal=500 COVID19=125	2	DarkCovidNet	98.08
		Normal=500 COVID19=125 PNEUMONIA=500	3		87.02
Ref [11]	Chest X-ray	Normal=1341 COVID19=3875	2	(IRRCNN) with Transfer Learning	84.67
	CT scan	Normal=247 COVID19=178			98.78
Ref [12]	CT scan	COVID19 (+) =1773 Non-COVID19 (-) =2221	2	ResNet18 with transfer learning and data augmentation	99.4
Ref [13]	CT scan	COVID19 (+) =345 Non-COVID19 (-) =397	2	ResNet50 + data augmentation and CGAN	82.91
Ref [14]	CT scan	Normal=8851 COVID19=238	2	Densenet-121 with transfer learning	96.49
		Normal=8851 COVID19=238	3		93.71

		PNEUMONIA=6045			
Ref [15]	Chest X-ray	Normal=1341 COVID19=864 PNEUMONIA=1345	3	DCNN + Inception V3 with transfer learning	93
Ref [16]	Chest X-ray	Normal=439 COVID19=435 BACTERIAL PNEUMONIA=439 VIRAL PNEUMONIA=439 TUBERCULOSIS=434	5	Resnet50 classifier	91.6
Ref [17]	Chest X-ray	Normal=310 COVID19=284	2	CoroNet	99
		Normal=310 COVID19=284 PNEUMONIA=667	3		95
		COVID-19=284 Normal=310 pneumonia bacterial=330 pneumonia viral=327	4		89.6
Ref [18]	Chest X-ray	Normal=504 COVID19=224 PNEUMONIA=714	3	CNN + Transfer learning	96.78
Ref [19]	Chest X-ray	Normal=50 COVID19=50	2	Transfer learning with Resnet50 and InceptionV3	98
Ref [20]	Chest X-ray	Normal=1050 COVID19=1050	2	CapsNet	97.24
Ref [23]	Chest X-ray	COVID19=183 Non-COVID19=13617	2	Faster R–CNN	97.36
Proposed study	**Chest X-ray**	**Normal=439 COVID19=435**	**2**	**our proposed CNN architecture model**	**99.7**
		Normal=1341 COVID19=864 PNEUMONIA=1345	**3**		**95.02**
		Normal=1341 COVID19=864 PNEUMONIA=1345 TUBERCULOSIS=434	**4**		**94.53**

References

[1] K. Purohit, A. Kesarwani, D. R. Kisku, and M. Dalui, "Covid-19 detection on chest x-ray and ct scan images using multi-image augmented deep learning model," BioRxiv, 2020.

[2] S. Hassantabar, M. Ahmadi, and A. Sharifi, "Diagnosis and detection of infected tissue of COVID-19 patients based on lung x-ray image using convolutional neural network approaches," Chaos, Solitons & Fractals, vol. 140, p. 110170, 2020.

[3] World Health Organization (WHO)

[4] "Coronavirus Disease 2019 (COVID-19) Symptoms". Centers of Disease and Control and Prevention. United States.

[5] Anosmia, Hyposmia, and Dysgeusia Symptoms of Coronavirus Disease". American academy of Otolaryngology-Head and neck surgery. 22 March 2020.

[6] C. Butt, J. Gill, D. Chun, and B. A. Babu, "Deep learning system to screen coronavirus disease 2019 pneumonia," Appl. Intell., p. 1, 2020.

[7] A. Abbas, M. M. Abdelsamea, and M. M. Gaber, "Classification of COVID-19 in chest X-ray images using DeTraC deep convolutional neural network," arXiv Prepr. arXiv2003.13815, 2020.

[8] H. Panwar, P. K. Gupta, M. K. Siddiqui, R. Morales-Menendez, and V. Singh, "Application of Deep Learning for Fast Detection of COVID-19 in x-Rays using nCOVnet," Chaos, Solitons & Fractals, p. 109944, 2020.

[9] M. Rahimzadeh and A. Attar, "A modified deep convolutional neural network for detecting COVID-19 and pneumonia from chest X-ray images based on the concatenation of Xception and ResNet50V2," Informatics Med. Unlocked, p. 100360, 2020.

[10] T. Ozturk, M. Talo, E. A. Yildirim, U. B. Baloglu, O. Yildirim, and U. R. Acharya, "Automated detection of COVID-19 cases using deep neural networks with x-ray images," Comput. Biol. Med., p. 103792, 2020.

[11] M. Z. Alom, M. M. Rahman, M. S. Nasrin, T. M. Taha, and V. K. Asari, "COVID_MTNet: COVID-19 Detection with Multi-Task Deep Learning Approaches," arXiv Prepr. arXiv2004.03747, 2020.

[12] S. Ahuja, B. K. Panigrahi, N. Dey, V. Rajinikanth, and T. K. Gandhi, "Deep transfer learning-based automated detection of COVID-19 from lung CT scan slices," 2020.

[13] M. Loey, G. Manogaran, and N. E. M. Khalifa, "A deep transfer learning model with classical data augmentation and cgan to detect covid-19 from chest ct radiography digital images," 2020.

[14] L. Sarker, M. M. Islam, T. Hannan, and Z. Ahmed, "COVID-DenseNet: a deep learning architecture to detect COVID-19 from chest radiology images," 2020.

[15] S. Asif, Y. Wenhui, H. Jin, Y. Tao, and S. Jinhai, "Classification of covid-19 from chest x-ray images using deep convolutional neural networks," medRxiv, 2020.

[16] A. H. Al-Timemy, R. N. Khushaba, Z. M. Mosa, and J. Escudero, "An efficient mixture of deep and machine learning models for covid-19 and tuberculosis detection using x-ray images in resource limited settings," arXiv Prepr. arXiv2007.08223, 2020.

[17] A. I. Khan, J. L. Shah, and M. M. Bhat, "Coronet: A deep neural network for detection and diagnosis of COVID-19 from chest x-ray images," Comput. Methods Programs Biomed., p. 105581, 2020.

[18] I. D. Apostolopoulos and T. A. Mpesiana, "Covid-19: automatic detection from x-ray images utilizing transfer learning with convolutional neural networks," Phys. Eng. Sci. Med., p. 1, 2020.

[19] A. Narin, C. Kaya, and Z. Pamuk, "Automatic detection of coronavirus disease (covid-19) using x-ray images and deep convolutional neural networks," arXiv Prepr. arXiv2003.10849, 2020.

[20] S. Toraman, T. B. Alakus, and I. Turkoglu, "Convolutional capsnet: A novel artificial neural network approach to detect COVID-19 disease from X-ray images using capsule networks," Chaos, Solitons & Fractals, vol. 140, p. 110122, 2020.

[21]https://www.kaggle.com/prashant268/chest-xray-covid19-pneumonia

[22]https://www.kaggle.com/raddar/chest-xrays-tuberculosis-from-india

[23] K. H. Shibly, S. K. Dey, M. T. U. Islam, and M. M. Rahman, "COVID Faster R-CNN: A Novel Framework to Diagnose Novel Coronavirus Disease (COVID-19) in X-Ray Images," medRxiv, 2020.

[24] M Gaata, W Puech, S. Sadkhan, S Hasson, "No-reference quality metric for watermarked images based on combining of objective metrics using neural network", 2012 3rd International Conference on Image Processing Theory, Tools and Applications (IPTA).

[25] S. B. Sadkhan, A. N. Abbas, "Watermarked and Noisy Images identification Based on Statistical Evaluation Parameters', Journal of Zankoy Sulaimani- Part A (JZS-A), 15 (3)